Available online at www.sciencedirect.com

SciVerse ScienceDirect

Procedia Food Science 1 (2011) 1165 – 1172

Procedia Food Science

11th International Congress on Engineering and Food (ICEF11)

On the use of combined heat flux measurements and image analysis procedures for the change of scale between industrial and pilot ovens

Alain Sommier[a]*, Yannick Anguy[a], Elisabeth Dumoulin[b], Juan Rojas[c], Marc Vignolle[c]

a I2M-TREFLE, UMR 5295, Espl des Arts et Métiers, 33405 Talence cedex, France (Alain.sommier@ensam.eu)
b Agroparistech, 1 avenue des Olympiades, 91744 Massy cedex, France
c Marie groupe LDC, 13-15 rue du Pont des Halles, 94526 Rungis, France

Abstract

Searching for optimal baking conditions for cereal products in industrial ovens by trial and error is a very costly process. Therefore, a procedure involving a change of scale is often needed, where the baking cycle can be optimized in a much smaller sized pilot oven. The quality and sensory attributes of baked cereal products are linked to the heat flux received by the product during baking. However, the net flux seen by the product can involve complex combinations of heat and mass transfer, chemical reactions and changes in the product over time. A tractable change of scale between the industrial oven and the pilot is based on a simpler flux measurement, which basically takes the process conditions into account. In this article we define baking conditions in the industrial line by measuring the convective and radiative fluxes received by commercial sensors lying on the conveyor belt amongst the products. We show that reproducing these fluxes in a small-sized pilot leads to products with similar color and mass loss to those in the industrial oven. This change of scale (down-scaling) means that baking conditions in the pilot can be optimized with respect to the product properties and the optimized baking cycle can then be replicated in the industrial oven (up-scaling). In order to validate this approach suitable tools are required to quantify the product properties. We highlight the use of image analysis to quantify macroscopic properties (e.g. color) and microscopic properties such as the size distribution of 3D air cells in the bread upon which sensory and mechanical properties depend.

Keywords: Heat flux measurement; baking; industrial oven; change of scale; cereal product microstructure

* Corresponding author. Tel.: +0556845415.
E-mail address: alain.sommier@ensam.eu.

2211–601X © 2011 Published by Elsevier B.V. Selection and/or peer-review under responsibility of 11th International Congress on Engineering and Food (ICEF 11) Executive Committee.
doi:10.1016/j.profoo.2011.09.174

1. Introduction

The food industry offers consumers a wide variety of products, which must be constantly and rapidly renewed, in order to keep up with customer expectations (e.g. food that is richer in fiber and/or low-fat) or European directives (e.g. reducing amounts of salt). This involves making changes to the original recipe and hence to the settings for the different transformation operations (mixing, fermentation, etc.). An essential stage in the production process is baking. Notably, this gives the product its familiar properties (texture, color, taste, volume, etc.). The time/temperature combination imposed on the product depends both on the product and the baking apparatus. Changes in the recipe will require adjustments to the heat settings for the oven. This adjustment stage is often carried out on a trial and error basis, which can lead to considerable product losses (an industrial oven typically contains 300 to 1,400 items). For this adjustment stage, it is essential to have a smaller-sized pilot oven and a way of scaling down from the industrial oven to the pilot. In this paper we show how direct measurement of the heat flux on the industrial production line [1-2] can be combined with measuring the product properties (e.g. color, mass loss) to apply a change of scale that reproduces the experimental conditions of the industrial oven in a small-sized pilot oven which can cook only one or two items. Because of this change of scale, it is then possible to carry out a more detailed study of the product and to optimize some of its properties (e.g. color). Looking further ahead, we present an application of X-ray microtomography [3-4] to measure properties in even more detail (e.g. statistics for 3D air cells), which will eventually enable us to optimize the product even further.

2. Materials and Methods

We devised a discontinuous ventilated instrument pilot oven to reproduce the thermal environment of an industrial tunnel oven. We added 10 kW heating elements to the pilot oven at the top and the bottom, retaining the original element and the fan at the back, for convection heating. Each element was coupled to a PID controller to regulate temperature to ± 1°C [5]. The product could be baked on a grill, a sheet, a mesh rack or a refractory concrete base. The concrete/resin oven base (custom-made by REFRACOIL, Paris, Fr), had a thermal conductivity of 0.74 $W.m^{-1}.K^{-1}$, and could therefore reproduce the contact conditions (product/tray) found in most industrial ovens. The mass loss kinetics was recorded relying on a weighing device under the tray rested on scales placed under the oven via a rod, which passed through the oven base. Control and data logging (temperature of the product, temperature of the oven, heat flux, pressure, humidity) were adjusted using a supervisory software that we had devised under labVIEW [5]. The flux sensors (Captec, Lille, Fr) were made from a surface thermopile placed on kapton film between 2 leaves of copper foil, on one of which there were constriction plots (Fig. 1). The upper part generated a temperature difference between the junctions of each thermocouple proportional to the thermal flux being measured. This was done by establishing thermal contact locally between one of the junctions of each thermocouple and the upper surface of the sensor (copper foil 35 µm thick). The sensor delivered a voltage that was proportional to the heat flux and to its size (about 5 $\mu v.W^{-1}.m^2$ for a 20x20mm sensor). The sensors were glued to a thermal assembly (Fig. 1) and measured total heat flux (black sensor) and convective flux (chrome sensor). The advantage of this device is that it provides direct measurement of the flux [2, 6] without having to then process the data. In this case the aluminium block had to be placed on an insulated support so that the sensor readings were not erroneous due to conductive flux contact.

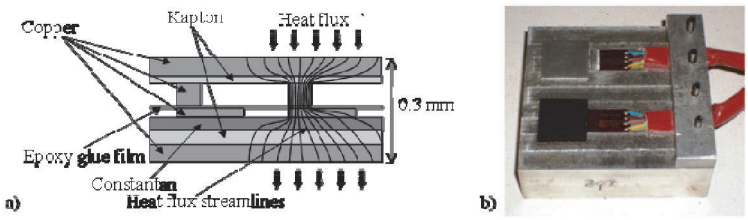

Fig. 1. a) Diagram showing section of flux sensor (Captec®). b) General view of sensors glued to a thermal assembly

The emissivity of the chrome sensor was close to 0. The flux Φ_{cr} (W.m^{-2}) measured by this sensor was essentially convective and is written $\Phi_{cr} \approx h_c(T_{air} - T_{cr})$, where h_c is the convective exchange coefficient (W.m^{-2}.K^{-1}), T_{air} is the air temperature in the oven above the sensors and T_{cr} is the temperature of the chrome sensor. The emissivity of the black sensor was close to 1. The flux Φ_b measured by this sensor was assimilated to total flux and is written $\Phi_b \approx h_c(T_{air} - T_b) + \sigma(T_{rad}^4 - T_b^4)$, where T_b is the temperature of the black sensor, σ is the Stefan-Boltzmann constant and T_{rad} is a radiation temperature assimilated to the temperature of the heating elements on the base and/or roof of the oven.

After a detailed study of the pilot oven (thermal and *flumetric* imaging), we produced some tables of reference to produce a heating cycle in the pilot, which gave products equivalent to those from the industrial line. Fig. 2 shows the change of scale in a case where the flux measured in the industrial oven was essentially convective.

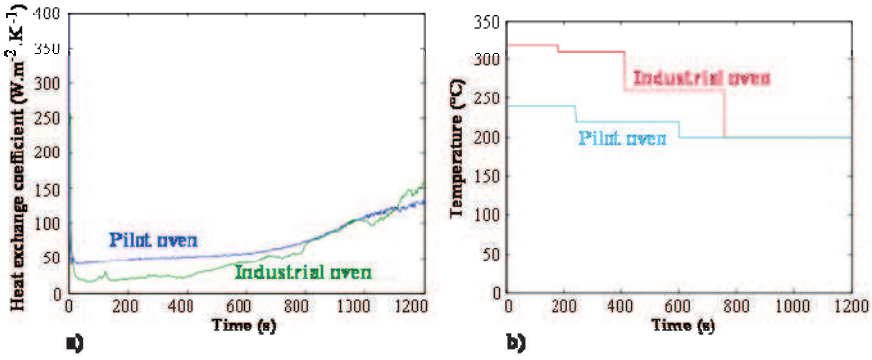

Fig. 2. a) Convective heat exchange coefficients $h_c = \Phi_{cr}/(T_{air} - T_{cr})$ measured in the pilot oven and in an industrial *impingement* tunnel oven. **b)** By using the convective temperature setting $T_{air}(t)$ in the pilot oven ("pilot oven" curve), we obtained a similar convective flux to that measured on the industrial production line.

The idea behind the change of scale was to juggle with the temperature setting T_{air} in the pilot oven over time (Fig. 2b) to obtain a convective flux during the baking process that was comparable to that measured on the industrial production line. More generally, we were trying to reproduce in the pilot oven the ratio observed over time on the industrial production line between the radiative and convective fluxes by adjusting the temperature setting T_{air} and the radiative temperature T_{rad} of the heating elements on the floor and the roof of the oven. To do this, we usually started by setting the majority flux and then refining by adjusting the minority flux.

3. Results and Discussion

We used an industrial air impingement tunnel oven (also called a hot air jet oven), indirect type, which included 4 modules, and was used to bake cereal products (quiches, tarts or pies). After putting the black and chrome sensors in place (Fig. 1) among the products, heat fluxes were measured for 1200 seconds (Fig. 3) across the 4 sections of the oven where the adjustable temperature settings (T_{air}) were set at 320, 310, 260 and 220°C respectively ("industrial oven" curve in Fig. 2b). Apart from one isolated increase at t=180s (caused by a poor contact in the casing for air circulation in the oven roof), the total flux Φ_b perceived by the black sensor at the top of the oven varied between 6000 and 3500 W.m^{-2} between sections 1 and 4 (Fig. 3a). Radiative flux (Φ_b - Φ_{cr}) made little contribution, about 30% to 5% of total flux, reaching a maximum value (2000 W.m^{-2}) in section 1 with the highest temperature setting (320°C). The majority of the flux was convective, as was to be expected in a hot air jet oven.

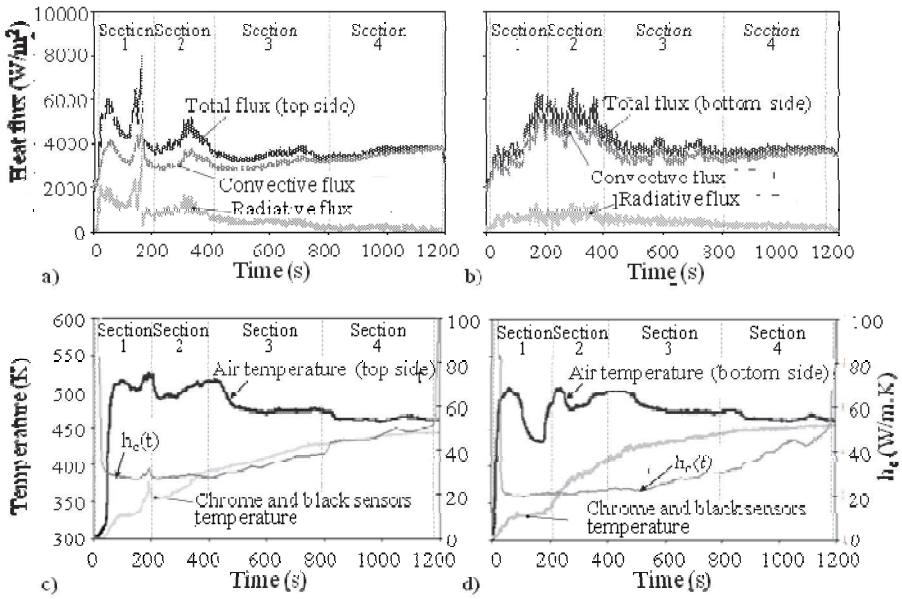

Fig. 3. Flux measurements received by sensors on the top (a) and the bottom (b) and calculated values for convective exchange coefficient $h_c(t)$ (c and d) for the industrial impingement oven

Calculating the convective exchange coefficient $h_c(t)$ ($h_c = \Phi_{cr}/(T_{air} - T_{cr})$) gave values of between 20 and 50 W.m^{-2}.K^{-1} (Figs. 3c-d) for this industrial oven. The same flux sensors were used to measure $h_c(t)$ in the pilot oven (Fig. 2a). In this example, the change of scale consisted of adjusting the temperature setting in the pilot oven (Fig. 2b) to obtain a convective flux during baking that was comparable to that measured on the industrial production line. We do not hypothesise here (as we do not need to) that the fluxes perceived by the sensors are the same as those perceived by the products (different factor of shape, product changes in the course of the cooking process, etc.). We simply ensured that the black and chrome sensors perceived the same fluxes in both ovens. Given that this was the case, we supposed that the products also perceived the same fluxes in both ovens, even though these may be different fluxes from those received by the sensors. To validate or *finalise* the procedure (to validate this apparently plausible hypothesis), we needed to check that the properties of the products from the pilot oven and the industrial production line were identical. We based our analysis on simple image analysis

techniques to quantify some of the familiar product properties. For color, we perfected a means of taking images under controlled lighting conditions. The images were taken using a camera with a fixed focal distance [7]. The red channel of the RGB image (24 bits) was used as an 8-bit greyscale image where each pixel had a value between 0 (black) and 255 (white). In order to compare different products in terms of color, we selected a threshold value beyond which a pixel was considered to be colored. Binarization of the image on the basis of this threshold (chosen in consultation with the sensory expert) gave us a simple way of determining a percentage (%) of colored surface (Fig. 4a).

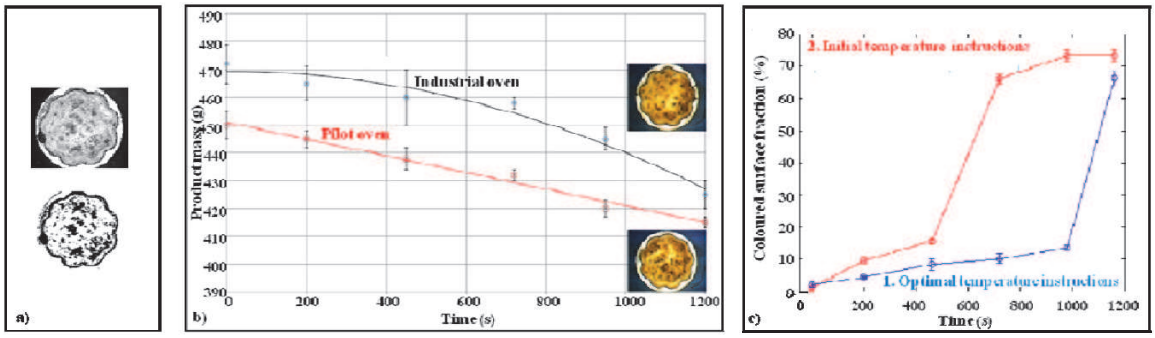

Fig. 4. a) Quantification of product color by image analysis (top: grey level image of the product; bottom: binary image, colored parts in black). b) Change of scale from the industrial line to the pilot oven. The products obtained in the two ovens with the baking conditions shown in Fig. 2 are comparable with respect to color and mass loss. c) Change of scale from the pilot to the industrial line. Colored product (quiche Lorraine) surface % *vs.* baking time for different temperature settings in the industrial oven. Curve 1: Optimal thermal cycle where the temperature settings in the 4 sections of the industrial line are 310, 310, 240 and 220°C, respectively. Curve 2: Initial thermal cycle: 320 - 310- 260 - 240°C (cf. "industrial oven" curve in Fig. 2b)

Figure 4b shows that in both ovens the change of scale produces comparable products in terms of mass loss and color. As changing scale from the industrial line towards the pilot oven (down-scaling) has been validated, we can then optimize the baking process in the pilot oven by trying, for instance, to optimize mass loss or color. The optimal conditions found in the pilot oven could then be transferred to the industrial line by carrying out the reverse procedure (up-scaling). Figure 4c shows that the color produced in an optimized baking cycle in the pilot oven (temperature settings lowered) is comparable to that obtained via an initial baking cycle in the industrial line, which consumes more energy (higher temperature settings).

In the food processing industry, only a limited number of studies have analyzed the structure of the product in very close detail [3-4, 8]. Following on from this article, we intend to apply X-ray micro-tomography to determine the 3D air cell space statistics for bread. This type of information, obtained by quantitative and automatic image analysis at a microscopic scale, is interesting in two respects for the procedure described above: (1) Direct comparison of the microstructure of different products and quantification of the impact of the formulation or the process on the structure of the final product, and (2) Access to microscopic information, which explains in part, or in full, a certain number of macroscopic properties of products hence ultimately a better understanding of the product.

Bread samples measuring a few cm^3 were imaged using X-ray microtomography to a spatial resolution of 12µm. The size of the elementary *voxel* (a *voxel* is the 3D equivalent of a TV *pixel*) was therefore 12x12x12 μm^3. Remember that data acquired from X-ray tomography are a series of projected images (2D) corresponding to different angular positions of the sample (here 2000). Using a filtered back-projection algorithm [9], the series of projections is transformed into a 3D image where each voxel of coordinates x, y, z has a grey level which is a function of the density and atomic number Z of the material(s) present in a volume 12x12x12μm^3 centered in x, y, z. Quantifying the 3D air cells in this type

of image involved an image analysis sequence under *Aphelion Developer,* illustrated in Fig. 5 in 2D for easier readability. Figure 5a is a 2D section taken from a 3D image reconstructed according to the protocol described above. To quantify the microstructure of this 8-bit image (grey levels between 0 and 255), the image is *segmented* (i.e. transformed into a binary image where the pixels that correspond to the solid matrix take a single value, 0 for example, and the pixels describing the voids equal 1, for example). The threshold value required for segmentation is sought automatically by maximizing the entropy of the grey levels histogram in Fig. 5a. The *level set* corresponding to the threshold obtained (87) is superimposed on the image in the close-up in Fig. 5a. Any pixel with a grey level or *altitude* higher (*resp.* lower) than 87 is considered to be part of the bread (*resp.* air) and set at 0 (*resp.* at 1). Figure 5b, where the air voids (1) are in red and the bread (0) in black represents the resulting binary image. Before quantifying the size and shape of the air cells, the cells in Fig. 5b that are partially overlapping have to be separated. The result of this, based on the *watershed* transformation, is shown in Fig. 5c where the cells are perfectly disassociated.

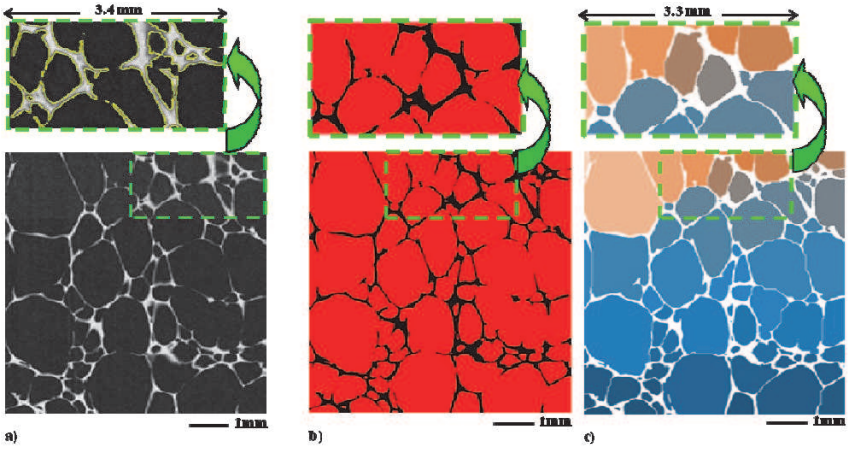

Fig. 5. a**)** 2D image in grey levels taken from a 3D image of a bread sample. Image size: 550x550 12µm pixels. In the close-up of Fig. 5a, see the level set (grey level equal to 87) used to transform Fig. 5a into the binary image shown in **b)**. In Fig. 5b, pixels with a value ≥ 87 (*resp.* < 87) which represent bread (*resp.* air) are put at a value 0 (*resp.* 1) and shown in black (*resp.* red). **c)** Individual disconnected cells. Each cell is identified using an arbitrary allocated label

The image analysis strategy shown in 2D is then applied in 3D (Fig. 6)

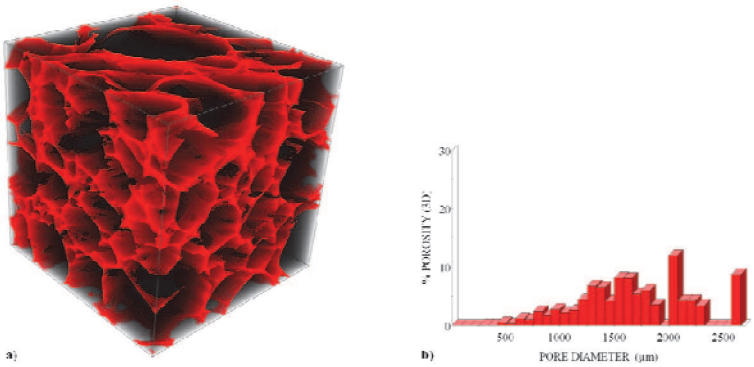

Fig. 6. a) Binary 3D image of bread obtained using the same protocol that produced Fig. 5b. Image size: 550x550x550 voxels (12µm), or 6.6x6.6x6.6mm^3. The bread matrix is shown in red. The porosity cells are transparent. **b)** Size distribution of the diameter of the 3D air cells (after separating overlapping cells (cf. Fig. 5c) and eliminating cells cut off at the edges of the image)

Figure 6a shows the binary 3D image obtained at the end of the segmentation stage (cf. Fig. 5b in 2D). 3D porosity was 89% and the specific surface was 1300 m^{-1}. Figure 6b gives the size distribution of the diameter of the 3D air cells (i.e. the % of 3D porosity associated with cells of a given diameter). The average diameter of the 3D air cells is 1700µm. To stabilize this statistical distribution, calculations were made on several sub-volumes of the type shown in Fig. 6a taken from the sample, which was several cm^3 in size. Many of the mechanical/sensory properties of cereal products depend on cell structure [4]. By quantifying this cell structure using modern image analysis techniques (Fig. 6) it is possible that in future we will be able to add more properties (influencing the customer choice) to the change of scale procedure, and thus optimize the baking process even further. Clearly, the multi-scale nature of cereal products [8] makes it more complicated to obtain representative statistics. The idea here was to show that methods do exist to quantify cell shape and size. In future, these image analysis methods will be combined with specially adapted sampling strategies so that the heterogeneity of these products and its impact on the sensory and mechanical properties of cereal products can be better taken into account [4, 8].

4. Conclusions

We show that convective and radiative thermal fluxes measured using commercial sensors on an industrial baking production line can be reproduced in a small-sized pilot by adjusting the pilot temperature settings. This down-scaling does not require the heat flux perceived by the sensor to be the same as the flux perceived by the product but rather supposes that if an industrial sensor (placed amongst the products on the conveyor belt) perceives an identical flux in both ovens, then the cereal products also receive a comparable flux, although it may be different from that perceived by the sensor. To verify this hypothesis, we used the direct link between the organoleptic / familiar properties of the baked product and the flux received during baking. We have shown that reproducing the flux measured by our sensors in an air jet industrial oven in the pilot oven gives similar coloring and mass loss in both. By downscaling we were then able to use the pilot oven to search quickly and at little cost for optimal baking conditions in terms of product properties. As an example, we used the pilot to determine an optimal baking cycle, reducing the amount of energy yet without changing the color. The repercussions for the industrial production line (up-scaling) of the optimized recommendations in the pilot gave a similar color. In future we hope to integrate more product properties into this procedure: not only color and mass loss, but also sensory and mechanical properties. These depend on the cell structure of the product at a very fine scale. We show that modern image analysis techniques can be used to quantify cell structure, which should in turn enable us to include more properties than in the past into this process of changing scales to optimize the production of baked goods.

References

[1]] Douiri I. 2007. Instrumentation d'un four pour la cuisson de la génoise. PhD Génie des procédés, Agroparistech, Massy, France.

[2] Fehaili S., Courel M., Rega B. & Giampaoli P. 2010. An instrumented oven for the monitoring of thermal reactions during baking of sponge cake. Journal of Food Engineering, 101(3), 253-263.

[3] Babin P., Della Valle G., Dendievel R., Lassoued N. & Salvo L. 2005. Mechanical properties of bread crumbs from tomography based finite element simulations. Journal of Materials Science, 40, 5867-5873.

[4] Lassoued N., Babin P., Della Valle G., Devaux M.-F. & Réguerre A.-L. 2007. Granulometry of bread crumb grain: Contributions of 2D and 3D image analysis at different scale. Food Research International, 40, 1087-1097.

[5] Sommier A., Chiron H., Colonna P., Della Valle G. & Rouille J. 2005. An instrument pilot scale oven for the study of French bread baking. Journal of Food Engineering, 69(1), 97-106.

[6] Rojas J., Vignolle M., Sommier A. & Trystram G. 2008. Heat flux measurement through a food industrial oven. International Workshop Trend in Cereal Science and Technology Industrial Applications, Thessaloniki, Greece, 4-5 February, 2008.

[7] Rojas J., Vignolle M., Choquart V. & Sommier A. 2008. Caractérisation de la couleur de surface des quiches par analyse d'images. FurturVIEW, Grenoble, France, 4-5 December, 2008, p.49.

[8] Chaunier L., Chrusciel L., Delisée C., Della Valle G. & Malvestio J. 2008. Permeability and Expanded Structure of Baked Products Crumbs. Food Biophysics, 3, 344-351.

[9] Feldkamp L.A., Davis L.C. & Kress J.W. 1984. Practical cone-beam algorithm. Journal of the Optical Society of America A, 1(6), 612-619.

Presented at ICEF11 (May 22-26, 2011 – Athens, Greece) as paper MCF366.